JOURNAL OF MATERIALS SCIENCE **39** (2004) 4507–4514

Ceramic matrix composites derived from $CrSi_2$-filled silicone polycyclic network

M. A. SCHIAVON, I. V. P. YOSHIDA
*State University of Campinas (UNICAMP), Institute of Chemistry, CP 6154,
Campinas, SP, 13083-970, Brazil
E-mail: valeria@iqm.unicamp.br*

Ceramic matrix composites (CMC) were prepared by the active-filler-controlled polymer pyrolysis, using a siloxane polycyclic network filled with $CrSi_2$. The starting $CrSi_2$-filled polysiloxane was pyrolyzed in both nitrogen and argon atmospheres, up to 1450°C. During the pyrolysis in nitrogen atmosphere, the $CrSi_2$ particles reacted with N_2, and also with carbon from the preceramic polymer binder, still complete consumption of the filler particles. Such reactions led to a dramatic change in the composition and microstructure of the resulting ceramic monoliths, which displayed linear expansion of 1.7%. In argon atmosphere, the $CrSi_2$ particles acted as inert filler during the pyrolysis process. The final CMC compositions obtained in N_2 and Ar atmospheres were $Cr_{0.62}C_{0.25}N_{0.03}$-$Si_3N_4$-$Cr_3C_2$ and SiO_xC_y-SiC-$CrSi_2$, respectively. © *2004 Kluwer Academic Publishers*

1. Introduction

Polymer pyrolysis is a relatively new and very promising technique for processing of advanced ceramics in complex shapes [1]. The main advantages of such polymer-derived ceramics are the applicability of polymer-processing techniques, the homogeneity of the precursors on a molecular level, the low processing temperatures when compared to conventional powder sintering methods, and the possibility of synthesizing new compounds [2].

The formation of bulk ceramics from polymer precursors, however, is difficult to achieve due to the high volume shrinkage associated with the polymer-ceramic conversion, which leads to intrinsic microcracks. In order to reduce the shrinkage upon pyrolysis, suitable filler materials can be incorporated into the polymeric precursors. Two types of fillers may be chosen: "inactive filler", which remains inert during the pyrolysis, and "active filler", which reacts with the pyrolysis by-products and/or gas of the atmosphere to form carbides or nitrides at high temperatures. The process associated with the incorporation of the latter filler is called AFCOP (Active-Filler-Controlled Polymer Pyrolysis), and has been developed by Greil [3]. According to this approach, the polymer is partially filled with active powder particles, which after pyrolysis, under appropriated conditions, generate reaction-bonded composite ceramics of variable compositions and high dimensional stability. In the systems derived from inactive fillers, the intrinsic shrinkage and porosity formation, during the polymer-ceramic conversion, can be reduced, according to the filler volume effect [3, 4]. Employing reactive filler particles, the reactions between these particles and the decomposition products of the polymeric phase or the reactive gas atmosphere promote a volume expansion. Consequently, near-net shaped crack-free composites can be achieved, due to the compensation of the polymer shrinkage by the appropriate filler expansion [3]. Combinations of different polymers, fillers, and reactive atmospheres may result in a variety of novel ceramic composite materials. Indeed, a number of systems have already been investigated using polysiloxanes as preceramic polymers filled with different ceramic or metallic powders, which lead after pyrolysis, to silicon oxycarbide (SiO_xC_y) or oxycarbonitride ($SiO_xC_yN_z$)-based composites such as SiO_xC_y-SiC [5, 6], SiO_xC_y-TiC, $SiO_xC_yN_z$-TiC [7], $SiO_xC_yN_z$-Si_3N_4-Cr_3C_2 [3], SiO_xC_y-Mo_2C [8] and SiO_xC_y-NbC-Al_2O_3 [9].

The aim of the present work was to apply the AFCOP process to the preparation of ceramic matrix composites using a liquid polymeric precursor. $CrSi_2$-filled polysiloxane was prepared by mixing the silicide powder with liquid cyclosiloxanes, bearing Si-H and Si-vinyl groups, forming *in situ* the siloxane polycyclic netwotk (SPN) through hydrosilylation reaction. Such SPN has already been studied, and it is able to produce at 1000°C, a silicon oxycarbide glass with high amount of carbidic groups as well as a free carbon phase [5, 6, 10]. The pyrolysis of the $CrSi_2$-filled SPN was carried out up to 1450°C, in argon and nitrogen atmospheres, giving rise to novel ceramic matrix composites. These composites were characterized by thermogravimetric (TGA) and thermal differential (DTA) analyses, X-ray diffraction (XRD), scanning electron microscopy (SEM), Hg-porosimetry and density measurements. The relationships between composition and microstructure of the resulting composites are discussed.

0022–2461

2. Experimental

2.1. Sample preparation

A siloxane polycyclic network, SPN, used as preceramic polymer, was prepared by *in situ* hydrosilylation reaction between the siloxane cyclic oligomers 1,3,5,7-tetra-methyl-1,3,5,7-tetravinylcyclotetrasiloxane (D_4Vi) and 1,3,5,7-tetramethyl-1,3,5,7-tetracyclotetrasiloxane (D_4H) (Dow Corning), in stoichiometric amount, using a platinum divinylcomplex, 2–3% in vinyl terminated poly(dimethylsiloxane) (Pt-catalyst) (Hülls), in 1% in relation to the total mass. In order to obtain green bodies, 45 vol% of $CrSi_2$ powder (99 wt%, 230 mesh, Aldrich) was blended with 55 vol% of D_4H, D_4Vi and Pt-catalyst mixture (polysiloxane liquid precursor). The mixture was uniaxially pressed ($\sim$80 MPa) in a steel mould, and stabilization of the green bodies was achieved by thermal crosslinking reaction at 70°C, over a period of 2 h. Pyrolysis of the monolithic materials was carried out in a tube furnace—Edgcon 5P or in a Thermolyne F59340-CM (for final temperatures between 1200 and 1450°C), both equipped with an internal alumina tube, under argon or nitrogen flow ($\sim$100 mL/min), in a multi-step-heating schedule. A typical heating cycle involved heating to 200°C, at 5°C/min, holding at this temperature for 120 min; then a second ramp to 450°C, at 5°C/min, keeping the sample at this temperature for 120 min; and a third ramp to the final temperature, at 2°C/min, holding at this temperature for 120 min. Finally, the samples were cooled down to room temperature, at 2°C/min. All the experiments yielded monolithic and crack-free samples.

2.2. Sample characterization techniques

Skeletal densities were measured with a helium pycnometer (Micromeritics, model 1035) while for suitable rectangular bars, the bulk densities were calculated by the ratio of mass over volume. Open porosity was determined by the ratio bulk/skeletal densities, and the data were checked with the values obtained by high-pressure mercury intrusion. Pore size distribution was characterized by high-pressure mercury intrusion using a porosizer (Micromeritics, model 9320), with intrusion pressures up to 207 MPa, which corresponds to an effective working range of the pore radius from 360 μm to 6 nm.

Thermogravimetric analysis (TGA) was performed on a thermobalance (Perkin Elmer, model TGA7) and differential thermal analysis (DTA) was performed on a calorimeter (TA Instrument, model 2910). Both analyses were carried out under flowing argon or nitrogen (100 mL/min), with a heating rate of 10°C/min up to the maximum temperature.

Fourier transform infrared (FT-IR) spectra were recorded using a spectrometer (Bomem, model B100). These spectra were obtained in the transmission mode on KBr pellets, recording 32 scans with a resolution of 4 cm^{-1}.

X-ray diffraction (XRD) patterns were collected with a diffractometer (Shimadzu, model XD3A) using Cu Kα radiation ($\lambda = 0.15418$ nm) as incident beam.

Microstructural characterization was performed by scanning electron microscopy (SEM), (Jeol—JSM 6360LV and JSM T-300), operating with an accelerating voltage of 25 and 20 kV, respectively. The last instrument is also equipped with an energy-dispersive X-ray spectroscopy (EDS) Be-detector (Noran Instruments) allowing chemical analysis. Si and Cr mapping were recorded in the Kα lines at 1.79 and 5.45 eV, respectively.

3. Results and discussion

3.1. Characterization of the green compact body

Bulk and skeleton densities of the $CrSi_2$-filled SPN green body were 2.8 and 3.5 g/cm^3, respectively. These values give an open porosity of 20%. This porosity was due to the partial filling of the pores by the SPN preceramic polymer. These pores were formed by the agglomeration of irregular shape filler particles. SEM observations performed on the surface fracture of the green body showed a homogenous dispersion of the SPN polymer on the silicide powder particles, with good adhesion at the polymer particle interface, as can be seen in Fig. 1. The well-dispersed and continuous polymeric phase on the powder surface is easily achieved due to the low viscosity and surface tension of the siloxane precursors. SPN polymer was prepared via hydrosilylation reaction, which occurs between the Si-H, from D_4H, and Si—CH=CH_2, from D_4Vi, in the presence of Pt^{II} catalyst. In this addition reaction no by-product is formed [5]:

$$\underset{(D_4Vi)}{n[CH_3(CH{=}CH_2)SiO]_4} + \underset{(D_4H)}{n[CH_3(H)SiO]_4}$$

$$\xrightarrow{Pt^{II}} \underset{(SPN)}{[(CH_3SiO{-}CH_2{-}CH_2{-}OSiCH_3)_4]_n}$$

Indeed, SPN is a rubbery polycyclic silicone network [5], and its structural evolution to ceramic material was already fully investigated by ^{29}Si and ^{13}C MAS NMR, FT-IR, XRD and TGA techniques [5, 6, 10]. The hydrosilylation reaction was enable to incorporate more than 70% of reactive functions in the polysiloxane network, resulting in a high crosslinking density, making it useful for the CMC forming technology. SPN is an excelent precursor of SiO_xC_y, with 86% of ceramic yield, at 1000°C. In relation to Si sites distribution, this amorphous ceramic presents the following composition: SiO_4 (22%), SiO_3C (27%), SiC_2O_2 (21%) and SiC_4 (30%) [5, 6]. The amount of rich-carbidic sites such as SiC_4 and SiO_2C_2 is higher than those usually observed in glasses products obtained from the pyrolysis of alkoxysilane gels reported in literature, which consist primarily of SiO_4, SiO_3C [11]. The residual carbon content (free carbon) estimated by elemental analysis was 70 wt% (in relation to the total carbon).

3.2. Thermal analysis

TGA curves of SPN and $CrSi_2$-filled SPN samples on both argon and nitrogen atmospheres up to 1400°C are displayed in Fig. 2. The weight loss associated with

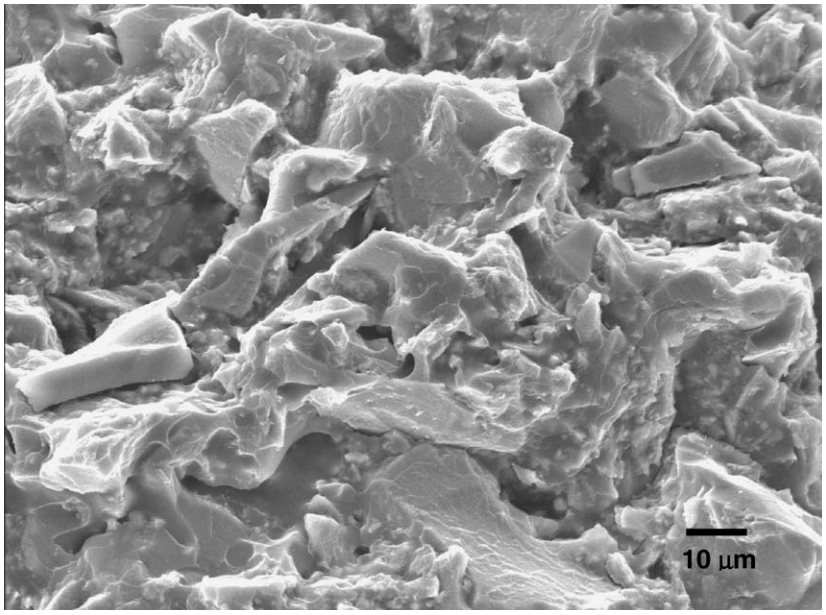

Figure 1 SEM micrograph of the surface fracture of the $CrSi_2$-filled SPN.

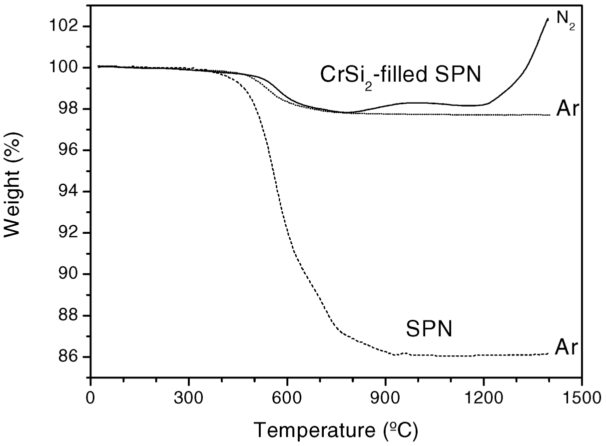

Figure 2 TGA curves recorded during pyrolysis of SPN under argon atmosphere and $CrSi_2$-filled SPN in nitrogen and argon atmospheres.

the SPN pyrolytic process started at 400°C. The high stability of SPN is due to the high degree of connectivity of this polycyclic network, which reduces the escape of siloxane volatiles, increasing the ceramic yield [10]. The temperature of initial weight loss in the $CrSi_2$-filled SPN sample was ~500°C, for both atmospheres. The temperature of maximum degradation, T_{Max}, was 560°C for SPN, and 565 and 571°C for $CrSi_2$-filled SPN, in argon and N_2 atmospheres, respectively. This is probably related to the residual porosity that entrapped volatile by-products, retarding their elimination. From 1000 to 1400°C, a rich-carbidic silicon oxycarbide glass was formed from SPN, and no significative weight change was detected, even if devitrification of the metastable phases (producing nanocrystalline SiC dispersed in an amorphous SiO_2 matrix) was observed by XRD [5]. The profiles of the $CrSi_2$-filled SPN, in both atmospheres, were very similar to that of SPN up to 800°C, with lower magnitude of the weight loss. A continuous stability up to 1400°C was observed under argon, which allows the $CrSi_2$ particles to be classified as an inactive filler. However, in nitrogen at 800°C, a slight weight gain was observed, and from 1200°C to higher temperatures, a continuous weight increase was registered. The $CrSi_2$-filled SPN composite gave rise to ceramic yields of 97.7 and 102.3 wt%, for argon and nitrogen atmospheres, respectively, at 1400°C. This weight gain in the nitrogen condition corresponds to the nitridation of the system.

In order to follow this nitridation process, DTA curves were recorded for the $CrSi_2$-filled SPN as well as for $CrSi_2$ and SPN, in argon (Fig. 3), and in nitrogen (Fig. 4) atmospheres. The intense exothermic peaks centered in the range of 200 to 400°C, in the SPN and $CrSi_2$-filled SPN samples, were associated with the thermally induced hydrosilylation reaction. The polysiloxane network rearrangements, which occur through degradation and redistribution reactions, were characterized by a larger exothermic process centered at 453°C for SPN and 547°C for the $CrSi_2$-filled SPN. This event was shifted to higher temperatures in the composite, which agrees with the increase in T_{Max} observed in TGA. Low intensity endothermic

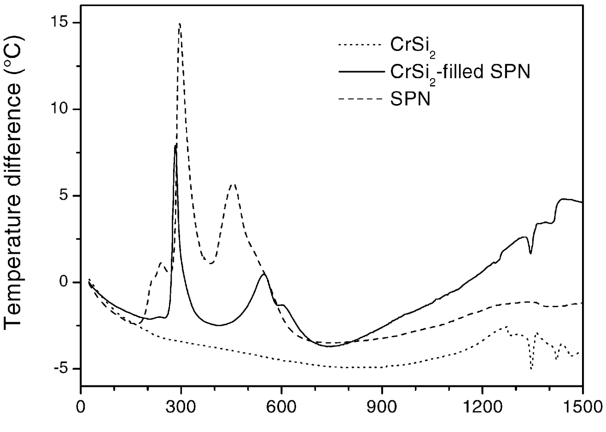

Figure 3 DTA curves recorded during pyrolysis in argon atmosphere of SPN, $CrSi_2$ and $CrSi_2$-filled SPN.

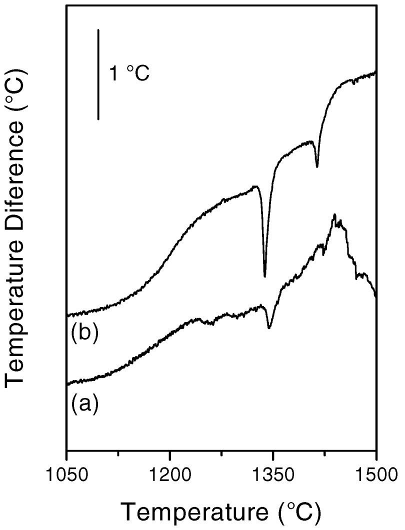

Figure 4 High-temperature DTA curves recorded in nitrogen atmosphere for: (a) $CrSi_2$-filled SPN; (b) $CrSi_2$.

peaks centered at 1275, 1346, 1421 and 1463°C, for the pure $CrSi_2$ filler, were associated with melting-recrystallization processes, involving crystals of different sizes and/or phase transition at high temperatures, near to the melting point of the main phase. In the $CrSi_2$-filled SPN these peaks were also observed, with less definition, due to the dilution effect promoted by the polymer-derived phase. Fig. 4 shows the high-temperature range of the $CrSi_2$-filled SPN and $CrSi_2$ curves obtained under nitrogen atmosphere. In the presence of N_2, only the most intense endothermic melting peaks at 1342 and 1414°C were observed for the $CrSi_2$. The last peak was associated with the melting of a recrystallized phase. In the $CrSi_2$-filled SPN, in addition to these peaks, a large exothermic event, centered at 1448°C was also observed. Such an event was associated with reactions between N_2 gas, $CrSi_2$ particles and carbon phase. It is interesting to note that for the pure $CrSi_2$ phase, no exothermic reaction was detected. The carbon phase present in the amorphous SiO_xC_y, derived from SPN polymer, had a crucial role as a carbon source for the formation of new ceramic phases.

3.3. Phase development

The phase development of the CMC samples was characterized by XRD, as can be seen in Fig. 5. The pyrolysis products obtained from $CrSi_2$-filled SPN in both atmospheres at 1000°C (not shown), as well as in argon atmosphere at 1200°C, showed XRD patterns characterized by the presence of peaks at 27.2, 36.7, 40.7, 42.6, 43.3, 50.5 and 73.3 (2θ), corresponding to the $CrSi_2$ hexagonal phase [12]. At 1450°C, in addition to the above diffractions, those characteristics of β-SiC, at 35.6, 60.0 and 72.0 (2θ) [12] were observed, due the reorganization of the SiC_xO_y phase [5, 10]. A new shoulder peak at 43.7 (2θ) is due to the carbon incorporation in $CrSi_2$, giving rise, according to ref. [13], to the $Cr_5Si_3C_x$ phase. Such incorporation was promoted by the dissolution of carbon in the fused filler [13]. No other crystalline phase was detected, suggesting that the $CrSi_2$ acted mainly as an inert filler, in argon atmosphere. However, in nitrogen atmosphere, at 1200°C the diffractions of the starting $CrSi_2$ were no more observed. Instead of this, in addition to $Cr_5Si_3C_x$, new crystalline phases were present, such as: silicon oxynitride, Si_2N_2O, α and β-Si_3N_4 and Cr_3C_2. The XRD peak assignments are in accordance with the refs. [3, 12–14]. The appearance of theses phases at this temperature, agreed with the observation of exothermic reactions in the DTA curve. At 1450°C, the formation of α- and β-Si_3N_4 and Cr_3C_2 were intensified, in addition to the chromium-carbon nitride, $Cr_{0.62}C_{0.35}N_{0.03}$, phase. The general reaction that describes the Si_3N_4 and Cr_3C_2 formation is:

$$3CrSi_{2(s)} + 2C_{(s,g)} + 4N_{2(g)} \rightarrow Cr_3C_{2(s)} + 2Si_3N_{4(s)} \qquad (1)$$

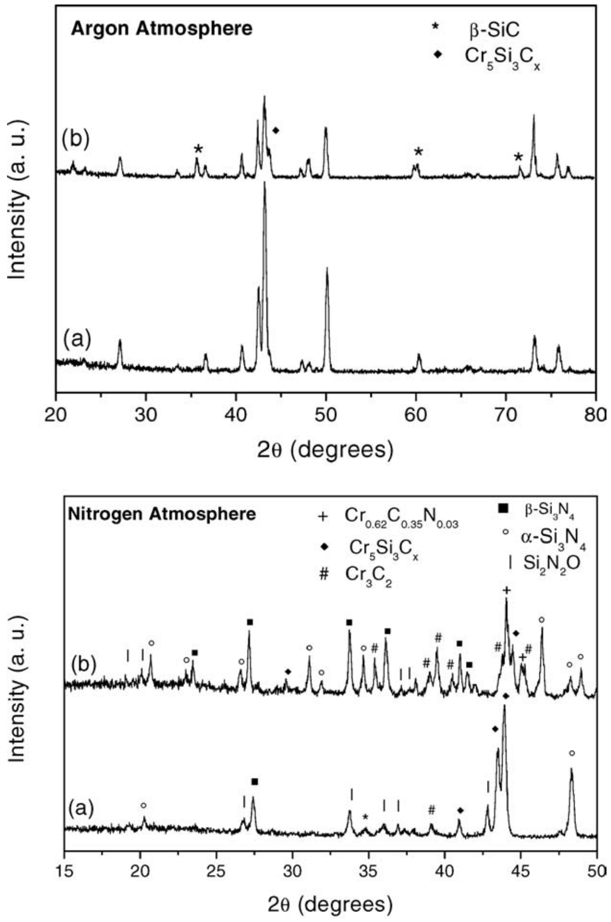

Figure 5 XRD patterns of the CMCs derived from $CrSi_2$-filled SPN in argon and nitrogen atmospheres pyrolysed at: (a) 1200°C; (b) 1450°C.

The FT-IR analyses matched the composition of the resulting CMCs. In the FT-IR spectra (not shown) of CMCs pyrolysed at 1000°C, two broad bands assigned to ν Si—O—Si and ν Si—C—Si absorptions, centered at 1080 and 800 cm^{-1}, respectively, appeared. Such bands are commonly observed in the SiO_xC_y glasses and confirm the existence of Si—C and Si—O bonds into the random network of these glasses [5]. In addition, a shoulder at ~1150 cm^{-1} assigned to ν Cr-Si bonds from $CrSi_2$ was also observed [15]. In the samples pyrolysed in nitrogen atmosphere at 1450°C, such bands disappeared and new broad absorptions centered at ~920 cm^{-1} and 800 cm^{-1}, associated to Si—N and Si—C bonds, respectively, were observed [16]. In contrast, for samples obtained in argon at 1450°C, the Si—O—Si band did not completely disappear. In conclusion, the resulting CMCs, obtained under nitrogen and argon, can be described as $Cr_{0.62}C_{0.35}N_{0.02}$-$Si_3N_4$-$Cr_3C_2$ and SiO_xC_y-SiC-$CrSi_2$, respectively.

3.4. Microstructure development

Bulk and skeleton densities were measured on samples pyrolyzed at various temperatures, ranging from 1000 to 1450°C. The density data together with the open porosity, linear shrinkage and ceramic yield values after pyrolysis are shown in Table I. Skeleton density values of the ceramic composites obtained under argon atmosphere increased with the pyrolysis temperature, due to the transformation of the polysiloxane (density 1.01 g/cm^3) to SiO_xC_y glass (density 2.19 g/cm^3), and finally to β-SiC (3.21 g/cm^3) [5]. This process resulted in a parallel increase of the porosity, since no significant difference in the bulk density was observed, which confirms the low reactivity of the $CrSi_2$ filler by pyrolysis in argon. On the other hand, the ceramic composites obtained by pyrolysis in nitrogen atmosphere, showed skeleton density values of 3.9 g/cm^3, independent of the pyrolysis temperature, while the bulk density value decreased at 1450°C, with consequent increase in the porosity value at this temperature. These results suggested that at 1450°C, substantial microstructural changes occurred, in addition to the compositional changes already discussed. The most important results in this table, however, are the changes observed in the values of ceramic yield and linear shrinkage. The increase in the weight and porosity values for the sample obtained at 1450°C led to a linear expansion of 1.7%, with the maintenance of the CMC shape. The polymer-derived ceramic phase gives rise to an infusible skeleton, which plays an important role in the microstructure of the CMC, allowing shape retention under appropriate experimental conditions.

The kinetics of the filler particle reaction has been described according to the shrinkage core model [17]. According to this model, by decreasing the filler particle size, the filler reaction time is reduced, and higher fractions of small particles are transformed, resulting in decreasing shrinkage. The present system fitted well in to such approach. Even though the $CrSi_2$ filler particles used were large (particle size <74 μm), they were completely transformed at 1200°C, under N_2 atmosphere, as seen by XRD. This fast consumption of the filler particles could be related to the open porosity observed in the green body (20%), where diffusion of volatiles as well as the nitrogen gas were facilitated.

TABLE I Ceramic yield, linear shrinkage, density and porosity values for the samples pyrolyzed in Ar and N_2 for 2 h

Temp. (°C)	Ceramic yield (%)	Linear shrinkage (%)	Density (g/cm^3) Bulk	Density (g/cm^3) Skeleton	Porosity (%)
		Argon atmosphere			
1000	97.8	2.1	3.6	4.3	16.3
1200	96.6	2.4	3.6	4.5	20.0
1450	93.4	3.6	3.6	4.7	23.4
		Nitrogen atmosphere			
1000	97.6	2.5	3.2	3.9	17.9
1200	100.4	0.7	3.2	3.9	17.9
1450	112.3	−1.7	2.9	3.9	25.6

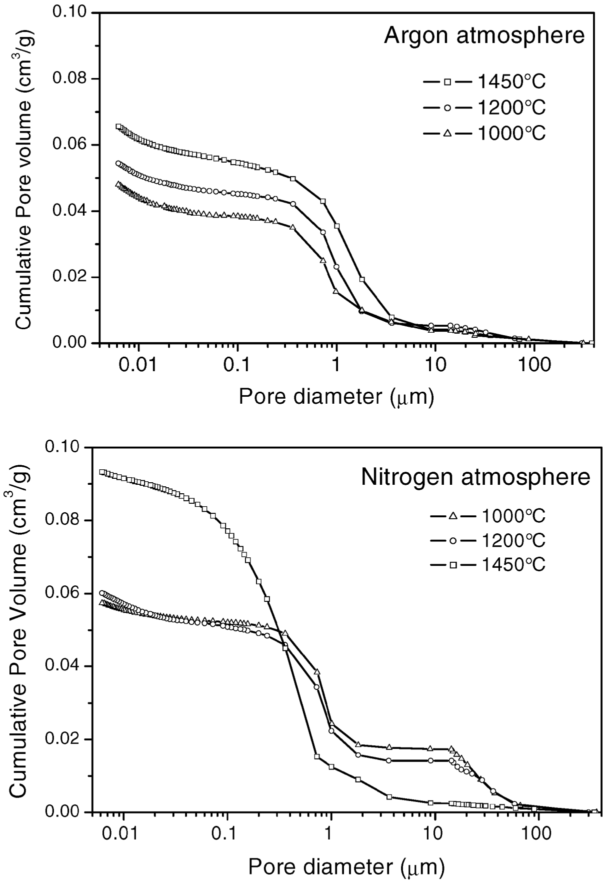

Figure 6 Cumulative pore volumes of $CrSi_2$-filled SPN pyrolyzed at 1000, 1200 and 1450°C in argon and nitrogen atmospheres.

The microstructure changes were also monitored by determination of the pore size distribution and SEM. The pore diameter distribution for all samples, shown in Fig. 6, was determined by high-pressure mercury intrusion. For the samples obtained by pyrolysis at 1000, 1200 and 1450°C, in argon atmosphere, the porosity increased with the temperature, displaying similar pore distributions. On the other hand, in nitrogen atmosphere, the samples pyrolyzed at 1000 and 1200°C displayed a similar pore distribution with diameters at ~20 μm and ~0.5 μm. However, at 1450°C, the pore size distribution was significantly changed, with a tendency to the formation of smaller pores.

Fig. 7 shows a typical microstructure of the $CrSi_2$-filled SPN pyrolyzed at 1450°C, in argon atmosphere. At this temperature the silicon oxycarbide matrix is above its glass transition temperature (T_g), known to be in the range of 1300–1350°C [18]. The viscous sintering of the glass matrix associated with the melted filler particles could close the smaller pores, increasing the densification. However, carbothermal reaction also occurs in the silicon oxycarbide matrix, which consumes

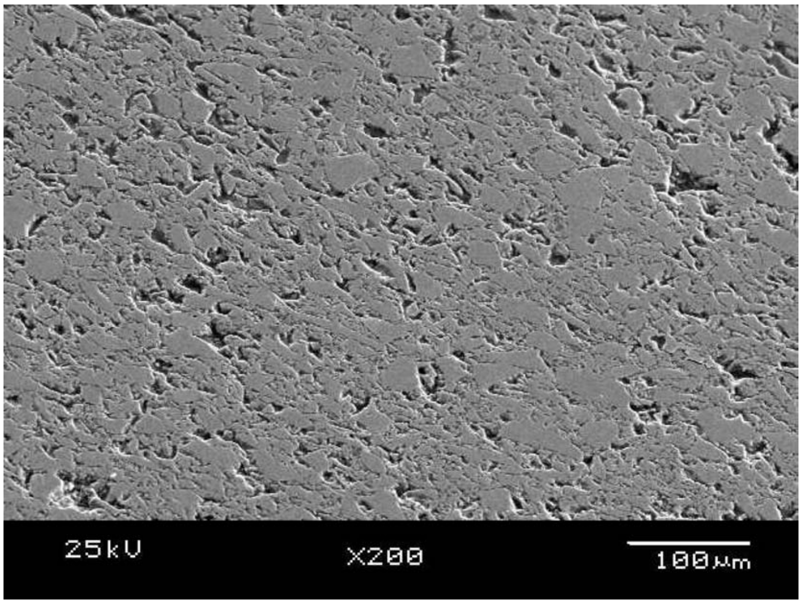

Figure 7 SEM micrograph of the fracture surface of the $CrSi_2$-filled SPN pyrolyzed at 1450°C, in argon atmosphere.

SiO_2 and C in the amorphous matrix to form SiC, releasing CO gas, which can explain the high open porosity for this composite. The global reaction, which describes the carbothermal reaction of the SiO_xC_y glass, is [19]:

$$SiO_{2(s)} + 3C_{(s)} \rightarrow SiC_{(s)} + 2CO_{(g)} \quad (2)$$

On the other hand, at 1450°C the grain boundary mobility is probably high, and the particle growth may result in a pronounced particle coarsening, which also leads to the formation of large pores.

The SEM micrographs of the fracture surfaces of $CrSi_2$-filled SPN, pyrolyzed at 1450°C in both atmospheres, are shown, at higher magnification, in Fig. 8. From the sample obtained in argon (Fig. 8A) it can be seen that a well-consolidated composite with continuity among the phases, the SiC_xO_y/SiC and the $CrSi_2/Cr_5Si_3C_x$ was produced. In samples pyrolyzed under nitrogen at 1000 and 1200°C (not shown), large cracks in addition to pores were observed. It seemed that in this temperature range grain growth also occurred, which could explain the large pores (bigger than 20 μm) observed in the pore size distribution. Indeed, in the DTA analysis, a weak endothermic peak at 1275°C was attributed to the filler softening, which could favor grain growth. At 1450°C (Fig. 8B), the $CrSi_2$-filled SPN showed a distinct morphology of a sample pyrolysed under argon. The pores were uniformly distributed in the CMC, and some larger pores still can be observed.

Scanning electron microscopy with energy dispersive X-ray spectroscopy (EDS) was also employed to obtain information about the microstructure of the resulting CMCs. In the microprobe analysis of the CMCs obtained in nitrogen atmosphere (not shown), Cr-rich regions in a continuous Si matrix were observed at 1450°C. This means that Cr-nano crystalline phases are present in a continuous α- and β-Si_3N_4 matrix. At 1200°C, much less obvious Cr and Si-phase segregation was observed.

According to the results of the present work, the method used here could be very useful for obtaining Cr_3C_2 in composites. This is worthwhile, since the synthesis of chromium carbide is usually by a reaction between Cr_2O_3 (74%) and C (26%), at 1600°C, in the presence of hydrogen, in a process where oxygen-free Cr_3C_2 with stoichiometric carbon content is difficult to obtain [20]. In addition, applying this method to the manufacture of complex shape hardfacing composites with higher chromium carbide contents could minimize the problem of machining since near net-shape CMCs can be obtained. Taking in account properties, such as high hardness, excellent wear resistance, low density and chemical stability [21], composites containing Cr_3C_2 have been reported as having improved mechanical and thermal properties then their pure phases. Indeed, the fracture toughness values of Al_2O_3/Cr_3C_2 composites were higher than that of monolithic Al_2O_3 [22].

The materials containing phases such as chromium silicide and silicon carbide, constitute a special class of materials of interest to the electronic industry. Silicon carbide is a preferred reinforcement phase in metal-silicide/silicon carbide composites because of its high elastic modulus, high thermal conductivity, small thermal expansion coefficient, high temperature strength, excellent shock resistance as well as semiconducting properties [15].

4. Conclusions

In the present work, ceramic matrix composites were prepared from $CrSi_2$-filled silicone polycyclic network, by using a processing route based on the active-filler controlled pyrolysis process (AFCOP). The main advantage of using this SPN was its *in situ* preparation, during the initial molding step, by hydrosilylation reaction, with no by-product formation, and high level of crosslinking. In addition, the liquid silicone precursor

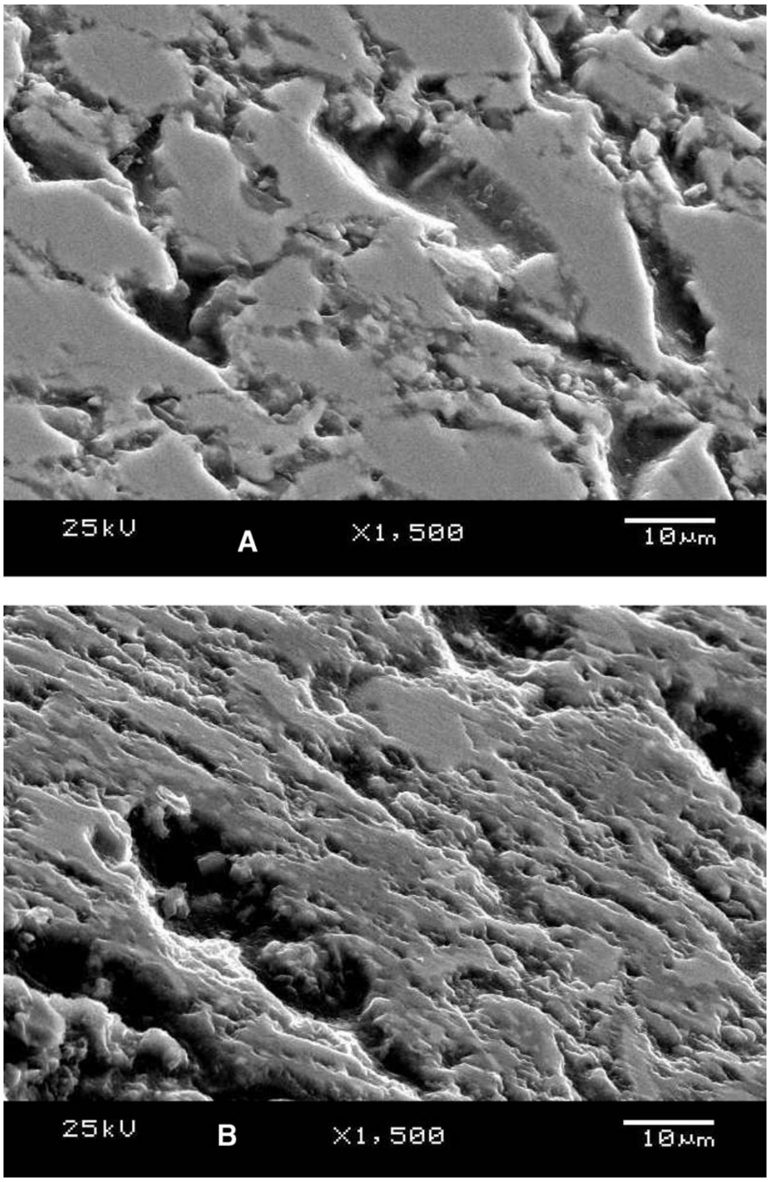

Figure 8 SEM micrographs (tilted 60 °) of the fracture surfaces of the $CrSi_2$-filled SPN pyrolyzed at 1450°C under: (A) argon atmosphere; (B) nitrogen atmosphere.

improved the homogeneous SPN distribution on the filler particles, resulting in a uniform microstructure of the green body.

The AFCOP method was successfully applied for the preparation of near-net shape $Cr_{0.62}C_{0.35}N_{0.03}$-$Si_3N_4$-$Cr_3C_2$ and SiO_xC_y-SiC-$CrSi_2$ composites, at 1450°C, by using both, nitrogen and argon atmospheres, respectively. Under argon atmosphere the silicide acted mainly as an unreactive filler, with no reactions detected by the techniques used. Under nitrogen atmosphere, nitrogen and carbon incorporation occurred by the reaction with the active filler, producing new crystalline phases. In spite of the large filler particle size, the porosity obtained in the green body allowed the gas diffusion rate to be high enough to consume completely the filler particles.

Acknowledgments

FAPESP is kindly acknowledged for the financial support (grant n° 98/07025-7)

References

1. P. GREIL, *Adv. Eng. Mater.* **2** (2000) 339.
2. Q. WEI, E. PIPPEL, J. WOLTERSDORF, M. SCHEFFLER and P. GREIL, *Mater. Chem and Phys.* **73** (2002) 281.
3. P. GREIL, *J. Amer. Ceram. Soc.* **78**(4) (1995) 835.
4. P. GREIL and M. SEIBOLD, *J. Mater. Sci.* **27** (1992) 1053.
5. M. A. SCHIAVON, E. RADOVANOVIC and I. V. P. YOSHIDA, *Powder Technol.* **123** (2002) 232.
6. M. A. SCHIAVON, L. C. PARDINI and I. V. P. YOSHIDA, *Key Eng. Mater.* **189** (2001) 48.
7. T. EMY, M. SEIBOLD, O. JARCHOW and P. GREIL, *J. Amer. Ceram. Soc.* **76**(1) (1993) 207.
8. A. KAINDL, W. LEHNER, P. GREIL and D. J. KIM, *Mater. Sci. Eng. A-Struct* **260** (1999) 101.
9. O. DERMOVSEK, J. C. BRESSIANI, A. H. A. BRESSIANI, W. ACCHAR and P. GREIL, *J. Mater. Sci* **35** (2000) 2201.
10. M. A. SCHIAVON, S. A. U. REDONDO, S. R. O. PINA and I. V. P. YOSHIDA, *J. Non-Cryst. Solids* **304** (2002) 92.
11. C. G. PANTANO, A. K. SINGH and H. ZHANG, *J. Sol-Gel Sci. Techn.* **14** (1999) 7.
12. Powder Diffraction File Search Manual, Joint Committee on Powder Diffraction Standarts (Swarthmore, 1973).

13. M. NAKA, J. C. FENG and J. C. SCHUSTER, *J. Mater. Synth. Proces.* **6**(3) (1998) 169.
14. P. LUO, P. R. STRUTT, O. F. DEVEREUX and H. K. GUPTA, *Mater. Sci. Eng.* **B31** (1995) 243.
15. P. LUO and P. R. STRUTT, *J. Mater. Sci.* **30** (1995) 3475.
16. M. A. SCHIAVON, G. D. SORARÙ and I. V. P. YOSHIDA, *J. Non-Cryst. Solids* **304** (2002) 304.
17. O. LEVENSPIEL, in "Chemical Reaction Engineering" (Willey, New York, 1972).
18. T. ROUXEL, G. MASSOURAS and G. D. SORARÙ, *J. Sol-Gel Sci. Techn.* **14** (1999) 87.
19. G. D. SORARÙ and D. SUTTOR, *ibid.* **14** (1999) 69.
20. "Ullmann's Encyclopedia of Industrial Chemistry," 5th ed. (Verlogsgesellschff, Weinhein, 1988), vol. A5.
21. S. K. KO, C. W. WON and I. J. SHON, *Scripta Mater.* **37**(6) (1997) 889.
22. J. L. HUANG, K. C. TWU, D. F. LII and A. K. LI, *Mater. Chem. Phys.* **51** (1997) 211.

Received 17 July 2003
and accepted 6 April 2004